Title

Chronic expression of interferon-gamma leads to murine autoimmune cholangitis with a female predominance

Journal

Hepatology, 64(4)

ISSN

0270-9139

Authors

Bae, Heekyong R
Leung, Patrick SC
Tsuneyama, Koichi
et al.

Publication Date

2016-10-01

DOI

10.1002/hep.28641

Peer reviewed

Published in final edited form as:

Hepatology. 2016 October ; 64(4): 1189–1201. doi:10.1002/hep.28641.

Chronic Expression of Interferon Gamma Leads to Murine Autoimmune Cholangitis with a Female Predominance

Heekyong R. Bae[1], **Patrick S.C. Leung**[2], **Koichi Tsuneyama**[3], **Julio C. Valencia**[1], **Deborah L. Hodge**[1], **Seohyun Kim**[1], **Tim Back**[1], **Megan Karwan**[5], **Anand S. Merchant**[6], **Nobuyuki Baba**[8], **Dechun Feng**[4], **Ogyi Park**[7], **Bin Gao**[4], **Guo-Xiang Yang**[2], **M. Eric Gershwin**[2], and **Howard A. Young**[1]

Heekyong R. Bae: baeh@mail.nih.gov; Patrick S.C. Leung: psleung@ucdavis.edu; Koichi Tsuneyama: tsuneyama.koichi@tokushima-u.ac.jp; Julio C. Valencia: valencij@mail.nih.gov; Deborah L. Hodge: hodged@csr.nih.gov; Seohyun Kim: seohyun0811@gmail.com; Tim Back: backt@mail.nih.gov; Megan Karwan: whangm@mail.nih.gov; Anand S. Merchant: anand.merchant@nih.gov; Nobuyuki Baba: n-baba@chp-kagawa.jp; Dechun Feng: dechun.feng@nih.gov; Ogyi Park: opark5@jhmi.edu; Bin Gao: bgao@mail.nih.gov; Guo-Xiang Yang: Gxyang@ucdavis.edu; M. Eric Gershwin: megershwin@ucdavis.edu; Howard A. Young: YoungHow@mail.nih.gov

[1]Cancer and Inflammation Program, Center for Cancer Research, National Cancer Institute-Frederick, and SAIC Frederick, Frederick, MD [2]Division of Rheumatology, Allergy and Clinical Immunology, University of California Davis School of Medicine, Davis, California [3]Department of Pathology and Laboratory Medicine, Institute of Biomedical Sciences, Tokushima University Graduate School, Japan [4]Laboratory of Liver Diseases, National Institute on Alcohol Abuse and Alcoholism, Rockville, Maryland [5]Laboratory of Animal Science, National Cancer Institute-Frederick, Frederick, Maryland [6]CCR Collaborative Bioinformatics Core, National Cancer Institute, Bethesda, Maryland [7]The Russell H. Morgan Department of Radiology and Radiological Science, Johns Hopkins University School of Medicine [8]Central Laboratory Kagawa Prefectural Central Hospital, Takamatsu, Japan

Abstract

In most autoimmune diseases the serologic hallmarks of disease precede clinical pathology by years. Therefore the use of animal models in defining early disease events becomes critical. Herein we have taken advantage of a “designer” mouse with dysregulation of interferon gamma (IFNγ) characterized by prolonged and chronic expression of IFNγ through deletion of the IFNγ 3′ UTR AU-rich element. These mice develop primary biliary cholangitis (PBC) with a female predominance that mimics human disease and is characterized by upregulation of total bile acids, spontaneous production of AMA, and portal duct inflammation. Transfer of CD4 T cells from ARE-Del−/− to B6/Rag1$^{-/-}$ mice induced moderate portal inflammation, and parenchymal inflammation, RNA-sequencing of liver gene expression revealed that upregulated genes potentially define early stages of cholangitis. Interestingly, upregulated genes specifically overlap with the gene expression signature of biliary epithelial cells in PBC, implying that IFNγ may play a pathogenic role in biliary epithelial cells (BEC) in the initiation stage of PBC. Moreover,

Correspondence to: Howard Young, Cancer and Inflammation Program, Center for Cancer Research, National Cancer Institute-Frederick, and SAIC Frederick, Frederick, Maryland 21702 USA; OR M. Eric Gershwin, M.D., Division of Rheumatology, Allergy and Clinical Immunology, University of California Davis School of Medicine, Davis, California 95616 USA.

The authors declare no competing financial interests.

differentially expressed genes in female mice have stronger Type I and II interferon signaling and lymphocyte-mediated immune responses and thus may drive the female bias of the disease. In conclusion, changes in IFNγ expression are critical for the pathogenesis of PBC.

Keywords

interferons; autoimmune diseases; sex-biased; MHC Class II; CD4 T cells

INTRODUCTION

As with most autoimmune diseases, PBC is female predominant and has a long latency period between detection of autoantibodies and the clinical appearance of immunopathology (1–4). Although there are clearly major defects in adaptive immunity, including dysregulation of multiple T and B cell pathways (5–11), there is significant evidence for the role of innate immunity in modulating and perhaps even initiating disease activity (12–17). Indeed, we have proposed that PBC is a multi-hit disease involving independent but overlapping immune pathways that interact at different stages of disease activity, ultimately leading to the clinical entity of severe portal inflammation with potential cirrhosis.

The role of IFN in autoimmunity is controversial, but a Th1 cell-mediated inflammatory response appears critical for loss of tolerance. In the study herein, we have taken advantage of a mouse in which there is a deletion of the IFN 3′ untranslated region (3′ UTR) AU-rich element, resulting in chronic IFN expression, and report here that these mice develop not only the classic histologic features of autoimmune cholangitis but more importantly, have a gender-differential bias as well as characteristic dysregulation of bile acids. We propose that interferon dysregulation, including an interplay between Type I and Type II interferons, leads to initiation of PBC and the female bias observed in the human disease.

MATERIALS AND METHODS

Generation of ARE-Del−/− mice

The generation of this strain has been previously described (18) and the phenotype has been described as including a mild lupus-like disease. However, we observed that sera from older mice appeared fatty and this led to the studies reported herein; two ARE-Del lines, derived from individual ES cell clones, were selected and backcrossed at least 10 generations onto C57BL/6 mice. After backcrossing, the genetic backgrounds were assessed at the DartMouse Speed Congenic Core Facility at the Geisel School of Medicine at Dartmouth. Animal care was provided in accordance with the procedures outlined in the “Guide for Care and Use of Laboratory Animals” (National Research Council; 2011; National Academy Press: Washington, D.C.).

Histopathology

Detail protocols of haematoxylin and eosin (H&E) staining, Sirius Red staining, Fontana-Masson staining, and histological scoring are described in the Supplemental Material.

Detection of serum anti-mitochondrial antibodies (AMA)

Serum AMA were detected using our standard enzyme-linked immune-sorbent assay (ELISA) against recombinant proteins of the pyruvate dehydrogenase complex-E2 subunit (PDC-E2), branched chain 2-oxo-acid dehydrogenase E2 subunit (BCOADC-E2) and 2-oxo-glutararte dehydrogenase E2 subunit (OGDC-E2) (19).

Total bile acid analysis (TBA)

TBA was analyzed using freshly collected serum and a Total bile acid Enzymatic Cycling Assay Kit (Diazyme, Poway, CA), according to manufacturer's protocols with modifications as described in the Supplemental Material.

RNA sequencing

Detailed protocols, including mRNA preparation, library construction, Illumina HiSeq2500 sequencing and data processing, are described in the Supplemental Material. The data set is available in the National Center for Biotechnology Information/Gene Expression Omnibus (GEO), entries GSE76309.

Adoptive cell transfer

Spleen cells were collected from 20 weeks old female ARE-Del−/− mice. Mononuclear cells were isolated and $CD4^+$ or $CD8^+$ T cells were purified by positive selection with microbeads and MiniMacs separation columns. 10-week-old female B6/$Rag1^{-/-}$ mice were used as recipients. 1×10^6 $CD4^+$ T cells, $CD8^+$ T cells or whole spleen mononuclear cells were transferred into recipient mice via tail vein injection.

Evaluation of pathological change in recipient mice

20 weeks after cell transfer, mice were sacrificed and liver collected for H&E staining. The histopathology was graded as: none inflammation (or bile duct damage); minimal inflammation (or bile duct damage); mild inflammation (or bile duct damage); moderate inflammation (or bile duct damage); and severe inflammation (or bile duct damage). Levels of IFN-, TNF-, IL-6, and MCP-1 in serum of recipient mice were measured with a cytokine bead array assay using the Mouse Inflammatory Cytokine Kit.

RESULTS

Portal and lobular inflammation, bile duct damage, fibrosis and granuloma formation in ARE-Del−/− mice with female dominance

Hepatic lesions from 20 wk old female ARE-Del−/− mice were noted to have moderate to severe portal lymphoid cell infiltration, whereas male ARE-Del−/− had only mild to moderate infiltration (Figure 1A). Furthermore, portal and lobular inflammation, small bile duct destruction, and granuloma formation were more severe in female ARE-Del−/− mice (Figure 1B). We further assessed the severity of these hepatic lesions based on unbiased quantification of frequency (Figure 1C). A Mann-Whitney statistical analysis of all ages of mice (8–10 wks old; n=4, 19–24 wks; n=8, over 40 wks; n=4) demonstrated that female ARE-Del−/− mice have higher frequencies of lymphocyte infiltration, damaged bile ducts

and granulomas than male ARE-Del−/− mice. Bile duct destruction correlated with age, indicating that bile duct damage occurs at a later stage of progression (Supplementary Figure 1). Based on Sirius Red staining (Figure 1D), mild fibrosis was observed in female ARE-Del −/− mice; the severity of fibrosis was substantially lower or not detectable in male ARE-Del −/− mice (data not shown).

Both AST and ALT levels were significantly increased in 20 wk old female ARE-Del−/− mice, although not as high as one finds in models of hepatitis (20). Male ARE-Del−/− mice had significance changes in the level of ALT as compared to control littermates but there was no significant changes in the level of AST (Supplemental Figure 2). Considering that ALT is exclusively in cytoplasm, while AST is in both mitochondria and the cytoplasm, this result suggests that female ARE-Del−/− mice may have critical damage in the mitochondria of target cells.

Female ARE-Del−/− mice produce anti-mitochondrial antibodies

Eight-10 wk old female ARE-Del−/− mice had readily detectable antibodies to PDC-E2, BCOADC-E2 and OGDC-E2 (Figure 2A). These data were recapitulated at 20 wks of age (Figure 2C). The dominant autoantibody was directed to PDC-E2. In contrast, 8–10 wk old male ARE-Del−/− mice had detectable antibodies to PDC-E2, but had no significant differences with controls with respect to autoantibodies to OGDC-E2 or BCOADC-E2 (Figure 2B). Interestingly, at 20 wks of age, there were no significant detectable AMA to any of the three epitopes in the male groups compared to controls (Figure 2D).

Total bile acids (TBA) are highly up-regulated in female ARE-Del−/− mice

In 8 wk old mice, female ARE-Del−/− mice had a mild elevation of TBA (25.8 ± 3.67 uM, n=4). There were no significant changes observed in male ARE-Del−/− mice (Figure 3A). In contrast, significantly higher levels of TBA were observed in 20 wk old female ARE-Del−/− mice (115.6 ± 11.71 uM of mean ± SEM, n=8) vs control littermates (3.8 ± 0.36 uM, n=9) were observed. Male ARE-Del−/− mice had relatively mild induction of TBA (19.12 ± 5.5 uM, n=8) compared to control littermates (1.9 ± 0.36 uM, n=8) (Figure 3B). Linear regression was performed to analyze the correlation coefficient of the serum TBA with histological scores of lymphocytic infiltration, bile duct damage and granuloma formation. In 8–10 wks, there was no correlation between TBA and the histological scores (Supplemental Figure 3A), whereas 20 wks old mice had a relatively significant correlation of TBA with portal inflammation (R=0.79), lobular inflammation (R=0.76), bile duct damage (R=0.80) and granuloma formation (R=0.91) (Supplemental Figure 3B). Skin hyperpigmentation, a characteristic feature of PBC, was increased in 20 wks old female ARE-Del−/− mice (Figure 3C), potentially via inadequate bile flow due to bile duct destruction. Male ARE-Del−/− mice had mildly or no increased skin hyperpigmentation, similar to that observed in ARE-Del+/− heterozygotes. Overall, the level of TBA was correlated with the level of skin pigmentation in both ARE-Del−/− and ARE-Del+/− mice (data now shown).

Female-specific disease progression is characteristic of ARE-Del heterozygotes

ARE-Del heterozygote mice have approximately 50% the level of circulating IFN compared to homozygous mice. We evaluated liver histology in heterozygous mice compared to female ARE-Del−/− mice (Figure 4A). Although overall image-based severity of hepatic lesion of female ARE-Del+/− was less than female ARE-Del−/−, the histological scores of inflammatory regions indicated that female ARE-Del+/− mice had portal tract lymphocytic infiltrates and biliary duct lesions similar to female ARE-Del−/− mice. In contrast, male ARE-Del+/− mice had a much lower severity in lesions, consistent with the hypothesis that female mice are more sensitive and/or are amplifying the IFN signaling pathway compared to male mice (Figure 4B and 4C). We further analyzed serum AMA (Figure 4D and 4E) and TBA (Figure 4F) of ARE-Del+/− mice. In 20 wk old mice, the level of AMA was significantly upregulated in female ARE-Del+/− but not male ARE-Del+/− mice, similar to that observed in ARE-Del−/− mice. Serum levels of TBA were mildly increased in female ARE-Del+/− mice and did not correlate with histologic scores, unlike the above the data on female ARE-Del−/− mice (Supplemental Figure 3C).

Gene expression signatures in ARE-Del−/− mice

A Venn diagram presentation of the data reflects that female ARE-Del−/− mice have 1118 differentially expressed genes compared to control littermates, and male ARE-Del−/− mice have 288 differentially expressed genes based on the criteria of > ±2 fold changes and FDR < 0.05 (Figure 5A). There are 258 genes commonly overexpressed by female and male ARE-Del−/− mice, demonstrating that the majority of genes from male ARE-Del−/− mice are differentially expressed compared to female ARE-Del−/− mice. A heat map generated from these overlapping genes demonstrates that female ARE-Del−/− mice have stronger expression of these genes (Figure 5B). Considering that male ARE-Del−/− mice have only mild to moderate pathology, these overlapping gene expression patterns of both female and male ARE-Del−/− mice suggest their involvement in the initiation of autoimmune cholangitis. To explore the possible mechanism, we performed a pathway analysis of these 258 genes using Ingenuity Pathway Analysis (IPA). In this analysis, IFNγ (*p*-value as 4.5×10^{-38}) and the IFNα receptor (*p*-value as 4.5×10^{-26}) were observed as top upstream regulators while IFN signaling was more predominant in female ARE-Del−/− mice (Figure 5C). Consistent with gene expression data, we further confirmed higher levels of serum IFNγ in female ARE-Del−/− vs male ARE-Del−/− mice (Supplemental Figure 4). There was also significant stronger induction of chemokines (MIG, IP-10 and MIP-1b) and cytokines (TNFα, IL-10 and IL-13) in female ARE-Del−/−, whereas other cytokines and chemokines were not significantly altered. The antigen presentation pathway was detectable as a top canonical pathway for the 258 overlapping genes (Figure 5D) and MHC-II genes were the most highly expressed genes in both male and female ARE-Del−/− mice (Table 1), indicating that this pathway is likely critical for the initiation of this disease.

Similarity of gene signatures between human and ARE-Del−/− mice

Gene expression analysis on liver biopsy tissues from PBC patients indicated that IFNγ signaling was significantly detectable in both early and late stage of disease (21–23). Most of all, upregulation of IFNγ signaling was more evident on chronic nonsuppurative

destructive cholangitis (CNSDC) and biliary epithelial cells (BEC) lesions dissected by laser capture microdissection (LCM). As BEC is known as the target cell in PBC, we compared the gene expression profile of this lesion with ARE-Del−/− mice. Using the full list of genes in PBC-BEC lesions biopsied from PBC patients (n=5) vs normal subjects (n=3), we analyzed 78 differentially induced genes and performed Gene Set Enrichment Analysis (GSEA) of these genes in the human subject data using gene sets from ARE-Del−/− mice. Noticeably, IFNγ was detectable as a top upstream regulator (p-value as 4.2×10^{-29}), and there was a significant enrichment of the human gene data in the data obtained from both male and female ARE-Del−/− mice (Figure 6A–B), suggesting that IFNγ may play a pathogenic role in BEC in the early stage of PBC disease. Based on the similar expression pattern of representative human genes (Supplemental Table 1), H2-Aa (HLA-DQA1) expression was one of most significantly induced genes in ARE-Del−/− mice. Nobuyuki *et al* reported that the protein expression of HLA-DQA1 was highly increased in BEC lesions from PBC patients (27) and MHC II locus were significantly associated with susceptibility to PBC (31, 34), thus our data constantly implies the importance of MHC class II expression in BEC for the initiation stage of PBC.

We performed Ingenuity pathway analysis (IPA) of 253 genes from Italian patient cohorts selected by pathway-based linear combination test (LCT) (24). Remarkably, we determined that IFNγ is identified as the top upstream regulator (p-value as 1.8×10^{-15}) in these genes (Supplemental Figure 5). Furthermore, based on recent GWAS studies (25–28), we performed pathway analysis of 26 genes (Supplemental Table 2) that have the most significant variants (p-value $\leq 1 \times 10^{-5}$), selected by the National Human Genome Research Institute (NHGRI) GWAS Catalog (29). Twenty one genes among the 26 genes were connected to IFNγ-mediated signaling and IFNγ was also consistently detectable as the top upstream regulator (p-value as 8.7×10^{-9}) as core networks were generated (Figure 6C). Among the top canonical pathways of these genes, T helper cell differentiation, dendritic cell maturation and B cell development were identified as highly significant, and these pathways strongly overlapped with those identified in female ARE-Del−/− mice (Figure 6D). Target DE genes from female ARE-Del−/− mice for each pathway are listed (Supplemental Table 3) and the gene network of these genes also indicated with Ifng, Ifnar, Tnf, Il-10, Il-1b as top upstream regulator genes. Moreover, T helper cell-mediated responses were specifically upregulated in these pathways and immunohistochemical staining with anti-CD4 and anti-CD8 antibodies consistently showed higher CD4 infiltration in CNSCD lesions of female ARE-Del−/− mice (Supplemental Figure 6). Thus, based on the gene expression pathway analysis, the mouse model presented here and the human disease strongly overlaps.

CD4 T cells are critical in the induction of cholangitis in ARE-DEL−/− mice

Transfer of CD4 T cells from ARE-Del−/− mice to B6/Rag1$^{-/-}$ mice induced moderate portal inflammation, and mild parenchymal inflammation, while bile duct damage and granuloma formation were minimally induced (Figure 7A). As the transfer of CD4 T cells produced similar histological phenotypes with that observed upon transfer of whole spleen cells, CD4 T cells may thus have a critical role in the pathological progression observed in ARE-Del$^{-/-}$ mice. In contrast, transfer of CD8 T cells resulted in minimal portal and

parenchymal inflammation with no visible effects on bile ducts and no granuloma formation. The level of serum IFN-, TNF-α, IL-6 and MCP-1 were consistently increased in mice receiving CD4 T cells or whole spleen cells (Figure 7B). In comparison mice receiving CD8 T cells did not have significant induction of IFN-, TNF-α and IL-6 compared with $Rag1^{-/-}$ mice, and only MCP-1 was enhanced similar to what was observed in mice receiving CD4 T cells.

DISCUSSION

The data reported herein demonstrate that chronic expression of IFNγ leads to a classic PBC-like disease with female gender dominance. A number of murine spontaneous and induced models have been reported that manifest features of human PBC (30–38). Clearly, no single model has fully mimicked the immunopathophysiology of human PBC and none hitherto have exhibited female dominance. Immunologically, PBC has long been recognized as reflective of Th1 mediated autoimmunity. Our data indicate that the Th17 pathway suppresses the accumulation of IFNγ producing cells in liver during the early phase of cholangitis, also supporting the hypothesis that IFNγ has a pivotal role in the early events in autoimmune cholangitis (39). ARE-Del−/− mice, the expression of MHC in the liver is a major canonical pathway seen in both male and female mice, indicating that IFNγ is critical for early stage of disease progression via enhancing MHC class expression.

Similar to a wide spectrum of autoimmune diseases, there is no convincing explanation or physiological mechanisms that account for the strong female predominance in PBC (40). Epidemiological studies in PBC have suggested that frequent exposure to environmental chemicals such as nail polish, chemicals found in tobacco smoke and use of hormone replacement therapies are significantly associated with an increased risk of PBC (41). Other risk factors implicated in female predominance of PBC include recurrent urinary tract infection in females, use of exogenous estrogens as well as an increased prevalence of reproductive complications (42, 43). These risk factors may work synergistically in accelerating loss of tolerance. Thus, we emphasize that it is not a genetic predisposition, but rather the pathology mediated through the interplay of interferons as described above that results in disease pathology. For example, one may postulate that during infection, or a chemical xenobiotic exposure, that there is a transient and local upregulation of IFN, which in the genetically susceptible host, will lead to loss of tolerance. Our data would imply that these events may occur individually over time, each leading to an upregulation of MHC on target tissue.

We focused on the female-specific pathways in ARE-Del−/− mice to investigate the mechanisms involved in disease progression. Gene expression analysis showed that the immune response was critically affected in female ARE-Del−/− mice, especially in macrophages, dendritic cells, natural killer cells, T and B cells. Importantly, T helper cell-mediated signaling is one of highly upregulate pathways in female ARE-Del−/− mice, but not in male ARE-Del−/− mice. Interestingly, recent GWAS studies also point out that potential PBC causing single nucleotide variants (SNV) were enriched in CD4 T cell signaling (4). Of note, IL12-JAK-STAT4 signaling in IL-12 stimulated T cells may drive gender-biased susceptibility to autoimmune diseases due to enhanced Th1 responses as it has

been reported that estrogen causes increased phosphorylation of STAT4 in an NOD mice model (44). Consistent with our findings, CD4 T cells infiltrated in hepatic inflammatory lesions based on analysis of PBC liver biopsies (4) and our cell transfer results also supported the model that CD4 T cells are critical for pathological progression of PBC. Therefore, our data suggest that IFNγ-induced Th1 response via CD4 T cell activation drives the gender-biased progression of PBC.

In summary, this work presents evidence for a pathogenic role of IFNγ in the early stages and in the progression of PBC. Considering the prominence of a female-specific bias in PBC disease progression, further studies are necessary to investigate the mechanism of sex-biased interferon signaling, its effect on lymphocyte-mediated immune responses and on the mechanisms involved in IFNγ mediated biliary epithelial cell death. Such studies will then lead to a rational approach towards intervention and treatment of this chronic inflammatory disease.

Supplementary Material

Refer to Web version on PubMed Central for supplementary material.

Acknowledgments

Financial Support: Funding supported in part by National Institutes of Health grant, DK090019 (MEG).

We are grateful to Ian Mackay for his review and comments on the manuscript. We thank Ryosuke Bessho and Hayato Baba for help with image analysis, Jinjung Choi, Charlotte Hanson and Michael Sanford for help with technical assistance. This research was supported by the Intramural Research Program of the NIH, Center for Cancer Research, National Cancer Institute. The authors declare no competing financial interests.

Abbreviations

3′-UTR	three prime untranslated region
3-α-HSD	3-alpha-hydroxysteroid dehydrogenase
ALT	alanine aminotransferase
AST	aspartate aminotransferase
G-CSF	granulocyte colony-stimulating factor
GM-CSF	granulocyte macrophage colony-stimulating factor
H&E	haematoxylin and eosin
KC	keratinocyte chemoattractant
LIF	leukemia inhibitory factor
LIX	LPS-induced CXC chemokine
MCP-1	monocyte chemoattractant protein-1
M-CSF	macrophage colony-stimulating factor

MHC	major histocompatibility complex
MIP-1α	macrophage inflammatory protein 1 alpha
MIP-1β	macrophage inflammatory protein 1 beta
Thio-NAD	thionicotinamide adenine dinucleotide
UDCA	ursodeoxycholic acid
MCP-1	monocyte chemotactic protein 1

References

1. Floreani A, Franceschet I, Perini L, Cazzagon N, Gershwin ME, Bowlus CL. New therapies for primary biliary cirrhosis. Clinical reviews in allergy & immunology. 2015; 48:263–272. [PubMed: 25331740]
2. Gershwin ME, Mackay IR, Sturgess A, Coppel RL. Identification and specificity of a cDNA encoding the 70 kd mitochondrial antigen recognized in primary biliary cirrhosis. J Immunol. 1987; 138:3525–3531. [PubMed: 3571977]
3. Kaplan MM, Gershwin ME. Primary biliary cirrhosis. N Engl J Med. 2005; 353:1261–1273. [PubMed: 16177252]
4. Webb GJ, Siminovitch KA, Hirschfield GM. The immunogenetics of primary biliary cirrhosis: A comprehensive review. Journal of autoimmunity. 2015
5. Beuers U, Gershwin ME, Gish RG, Invernizzi P, Jones DE, Lindor K, Ma X, et al. Changing nomenclature for PBC: From 'cirrhosis' to 'cholangitis'. Digestive and liver disease: official journal of the Italian Society of Gastroenterology and the Italian Association for the Study of the Liver. 2015
6. Dhirapong A, Yang GX, Nadler S, Zhang W, Tsuneyama K, Leung P, Knechtle S, et al. Therapeutic effect of cytotoxic T lymphocyte antigen 4/immunoglobulin on a murine model of primary biliary cirrhosis. Hepatology. 2013; 57:708–715. [PubMed: 22996325]
7. Huang W, Kachapati K, Adams D, Wu Y, Leung PS, Yang GX, Zhang W, et al. Murine autoimmune cholangitis requires two hits: cytotoxic KLRG1(+) CD8 effector cells and defective T regulatory cells. Journal of autoimmunity. 2014; 50:123–134. [PubMed: 24556277]
8. Li Y, Wang W, Tang L, He X, Yan X, Zhang X, Zhu Y, et al. Chemokine (C-X-C motif) ligand 13 promotes intrahepatic chemokine (C-X-C motif) receptor 5+ lymphocyte homing and aberrant B-cell immune responses in primary biliary cirrhosis. Hepatology. 2015; 61:1998–2007. [PubMed: 25627620]
9. Tomiyama T, Yang GX, Zhao M, Zhang W, Tanaka H, Wang J, Leung PS, et al. The modulation of co-stimulatory molecules by circulating exosomes in primary biliary cirrhosis. Cellular & molecular immunology. 2015
10. Tsuda M, Ambrosini YM, Zhang W, Yang GX, Ando Y, Rong G, Tsuneyama K, et al. Fine phenotypic and functional characterization of effector cluster of differentiation 8 positive T cells in human patients with primary biliary cirrhosis. Hepatology. 2011; 54:1293–1302. [PubMed: 21735469]
11. Wang L, Sun Y, Zhang Z, Jia Y, Zou Z, Ding J, Li Y, et al. CXCR5+ CD4+ T follicular helper cells participate in the pathogenesis of primary biliary cirrhosis. Hepatology. 2015; 61:627–638. [PubMed: 25042122]
12. Chang CH, Chen YC, Yu YH, Tao MH, Leung PS, Ansari AA, Gershwin ME, et al. Innate immunity drives xenobiotic-induced murine autoimmune cholangitis. Clinical and experimental immunology. 2014; 177:373–380. [PubMed: 24547942]
13. Chang CH, Chen YC, Zhang W, Leung PS, Gershwin ME, Chuang YH. Innate immunity drives the initiation of a murine model of primary biliary cirrhosis. PloS one. 2015; 10:e0121320. [PubMed: 25807531]

14. Chuang YH, Lian ZX, Tsuneyama K, Chiang BL, Ansari AA, Coppel RL, Gershwin ME. Increased killing activity and decreased cytokine production in NK cells in patients with primary biliary cirrhosis. Journal of autoimmunity. 2006; 26:232–240. [PubMed: 16730427]
15. Chuang YH, Lian ZX, Yang GX, Shu SA, Moritoki Y, Ridgway WM, Ansari AA, et al. Natural killer T cells exacerbate liver injury in a transforming growth factor beta receptor II dominant-negative mouse model of primary biliary cirrhosis. Hepatology. 2008; 47:571–580. [PubMed: 18098320]
16. Kawata K, Kobayashi Y, Gershwin ME, Bowlus CL. The immunophysiology and apoptosis of biliary epithelial cells: primary biliary cirrhosis and primary sclerosing cholangitis. Clinical reviews in allergy & immunology. 2012; 43:230–241. [PubMed: 22689287]
17. Lleo A, Bowlus CL, Yang GX, Invernizzi P, Podda M, Van de Water J, Ansari AA, et al. Biliary apotopes and anti-mitochondrial antibodies activate innate immune responses in primary biliary cirrhosis. Hepatology. 2010; 52:987–998. [PubMed: 20568301]
18. Hodge DL, Berthet C, Coppola V, Kastenmuller W, Buschman MD, Schaughency PM, Shirota H, et al. IFN-gamma AU-rich element removal promotes chronic IFN-gamma expression and autoimmunity in mice. Journal of autoimmunity. 2014; 53:33–45. [PubMed: 24583068]
19. Moteki S, Leung PS, Coppel RL, Dickson ER, Kaplan MM, Munoz S, Gershwin ME. Use of a designer triple expression hybrid clone for three different lipoyl domain for the detection of antimitochondrial autoantibodies. Hepatology. 1996; 24:97–103. [PubMed: 8707289]
20. Lafdil F, Wang H, Park O, Zhang W, Moritoki Y, Yin S, Fu XY, et al. Myeloid STAT3 inhibits T cell-mediated hepatitis by regulating T helper 1 cytokine and interleukin-17 production. Gastroenterology. 2009; 137:2125–2135. e2121–2122. [PubMed: 19686746]
21. Baba N, Kobashi H, Yamamoto K, Terada R, Suzuki T, Hakoda T, Okano N, et al. Gene expression profiling in biliary epithelial cells of primary biliary cirrhosis using laser capture microdissection and cDNA microarray. Transl Res. 2006; 148:103–113. [PubMed: 16938647]
22. Honda M, Kawai H, Shirota Y, Yamashita T, Kaneko S. Differential gene expression profiles in stage I primary biliary cirrhosis. Am J Gastroenterol. 2005; 100:2019–2030. [PubMed: 16128947]
23. Shackel NA, McGuinness PH, Abbott CA, Gorrell MD, McCaughan GW. Identification of novel molecules and pathogenic pathways in primary biliary cirrhosis: cDNA array analysis of intrahepatic differential gene expression. Gut. 2001; 49:565–576. [PubMed: 11559656]
24. Kar SP, Seldin MF, Chen W, Lu E, Hirschfield GM, Invernizzi P, Heathcote J, et al. Pathway-based analysis of primary biliary cirrhosis genome-wide association studies. Genes and immunity. 2013; 14:179–186. [PubMed: 23392275]
25. Hirschfield GM, Liu X, Xu C, Lu Y, Xie G, Gu X, Walker EJ, et al. Primary biliary cirrhosis associated with HLA, IL12A, and IL12RB2 variants. The New England journal of medicine. 2009; 360:2544–2555. [PubMed: 19458352]
26. Liu X, Invernizzi P, Lu Y, Kosoy R, Bianchi I, Podda M, Xu C, et al. Genome-wide meta-analyses identify three loci associated with primary biliary cirrhosis. Nature genetics. 2010; 42:658–660. [PubMed: 20639880]
27. Mells GF, Floyd JA, Morley KI, Cordell HJ, Franklin CS, Shin SY, Heneghan MA, et al. Genome-wide association study identifies 12 new susceptibility loci for primary biliary cirrhosis. Nature genetics. 2011; 43:329–332. [PubMed: 21399635]
28. Nakamura M, Nishida N, Kawashima M, Aiba Y, Tanaka A, Yasunami M, Nakamura H, et al. Genome-wide association study identifies TNFSF15 and POU2AF1 as susceptibility loci for primary biliary cirrhosis in the Japanese population. American journal of human genetics. 2012; 91:721–728. [PubMed: 23000144]
29. Welter D, MacArthur J, Morales J, Burdett T, Hall P, Junkins H, Klemm A, et al. The NHGRI GWAS Catalog, a curated resource of SNP-trait associations. Nucleic Acids Res. 2014; 42:D1001–1006. [PubMed: 24316577]
30. Irie J, Wu Y, Wicker LS, Rainbow D, Nalesnik MA, Hirsch R, Peterson LB, et al. NOD. c3c4 congenic mice develop autoimmune biliary disease that serologically and pathogenetically models human primary biliary cirrhosis. J Exp Med. 2006; 203:1209–1219. [PubMed: 16636131]

31. Katsumi T, Tomita K, Leung PS, Yang GX, Gershwin ME, Ueno Y. Animal models of primary biliary cirrhosis. Clinical reviews in allergy & immunology. 2015; 48:142–153. [PubMed: 25771770]
32. Oertelt S, Lian ZX, Cheng CM, Chuang YH, Padgett KA, He XS, Ridgway WM, et al. Anti-mitochondrial antibodies and primary biliary cirrhosis in TGF-beta receptor II dominant-negative mice. Journal of immunology. 2006; 177:1655–1660.
33. Salas JT, Banales JM, Sarvide S, Recalde S, Ferrer A, Uriarte I, Oude Elferink RP, et al. Ae2a,b-deficient mice develop antimitochondrial antibodies and other features resembling primary biliary cirrhosis. Gastroenterology. 2008; 134:1482–1493. [PubMed: 18471521]
34. Wakabayashi K, Lian ZX, Leung PS, Moritoki Y, Tsuneyama K, Kurth MJ, Lam KS, et al. Loss of tolerance in C57BL/6 mice to the autoantigen E2 subunit of pyruvate dehydrogenase by a xenobiotic with ensuing biliary ductular disease. Hepatology. 2008; 48:531–540. [PubMed: 18563844]
35. Wakabayashi K, Lian ZX, Moritoki Y, Lan RY, Tsuneyama K, Chuang YH, Yang GX, et al. IL-2 receptor alpha(−/−) mice and the development of primary biliary cirrhosis. Hepatology. 2006; 44:1240–1249. [PubMed: 17058261]
36. Wang J, Yang GX, Tsuneyama K, Gershwin ME, Ridgway WM, Leung PS. Animal models of primary biliary cirrhosis. Seminars in liver disease. 2014; 34:285–296. [PubMed: 25057952]
37. Wang JJ, Yang GX, Zhang WC, Lu L, Tsuneyama K, Kronenberg M, Vela JL, et al. Escherichia coli infection induces autoimmune cholangitis and anti-mitochondrial antibodies in non-obese diabetic (NOD). B6 (Idd10/Idd18) mice. Clinical and experimental immunology. 2014; 175:192–201. [PubMed: 24128311]
38. Zhang W, Sharma R, Ju ST, He XS, Tao Y, Tsuneyama K, Tian Z, et al. Deficiency in regulatory T cells results in development of antimitochondrial antibodies and autoimmune cholangitis. Hepatology. 2009; 49:545–552. [PubMed: 19065675]
39. Kawata K, Tsuda M, Yang GX, Zhang W, Tanaka H, Tsuneyama K, Leung P, et al. Identification of potential cytokine pathways for therapeutic intervention in murine primary biliary cirrhosis. PloS one. 2013; 8:e74225. [PubMed: 24040208]
40. Sun Y, Haapanen K, Li B, Zhang W, Van de Water J, Gershwin ME. Women and primary biliary cirrhosis. Clinical reviews in allergy & immunology. 2015; 48:285–300. [PubMed: 25241227]
41. Zhang H, Carbone M, Lleo A, Invernizzi P. Geoepidemiology, Genetic and Environmental Risk Factors for PBC. Dig Dis. 2015; 33(Suppl 2):94–101. [PubMed: 26641264]
42. Gershwin ME, Selmi C, Worman HJ, Gold EB, Watnik M, Utts J, Lindor KD, et al. Risk factors and comorbidities in primary biliary cirrhosis: a controlled interview-based study of 1032 patients. Hepatology. 2005; 42:1194–1202. [PubMed: 16250040]
43. Smyk DS, Rigopoulou EI, Lleo A, Abeles RD, Mavropoulos A, Billinis C, Invernizzi P, et al. Immunopathogenesis of primary biliary cirrhosis: an old wives' tale. Immunity & ageing: I & A. 2011; 8:12. [PubMed: 22136162]
44. Bao M, Yang Y, Jun HS, Yoon JW. Molecular mechanisms for gender differences in susceptibility to T cell-mediated autoimmune diabetes in nonobese diabetic mice. J Immunol. 2002; 168:5369–5375. [PubMed: 11994496]

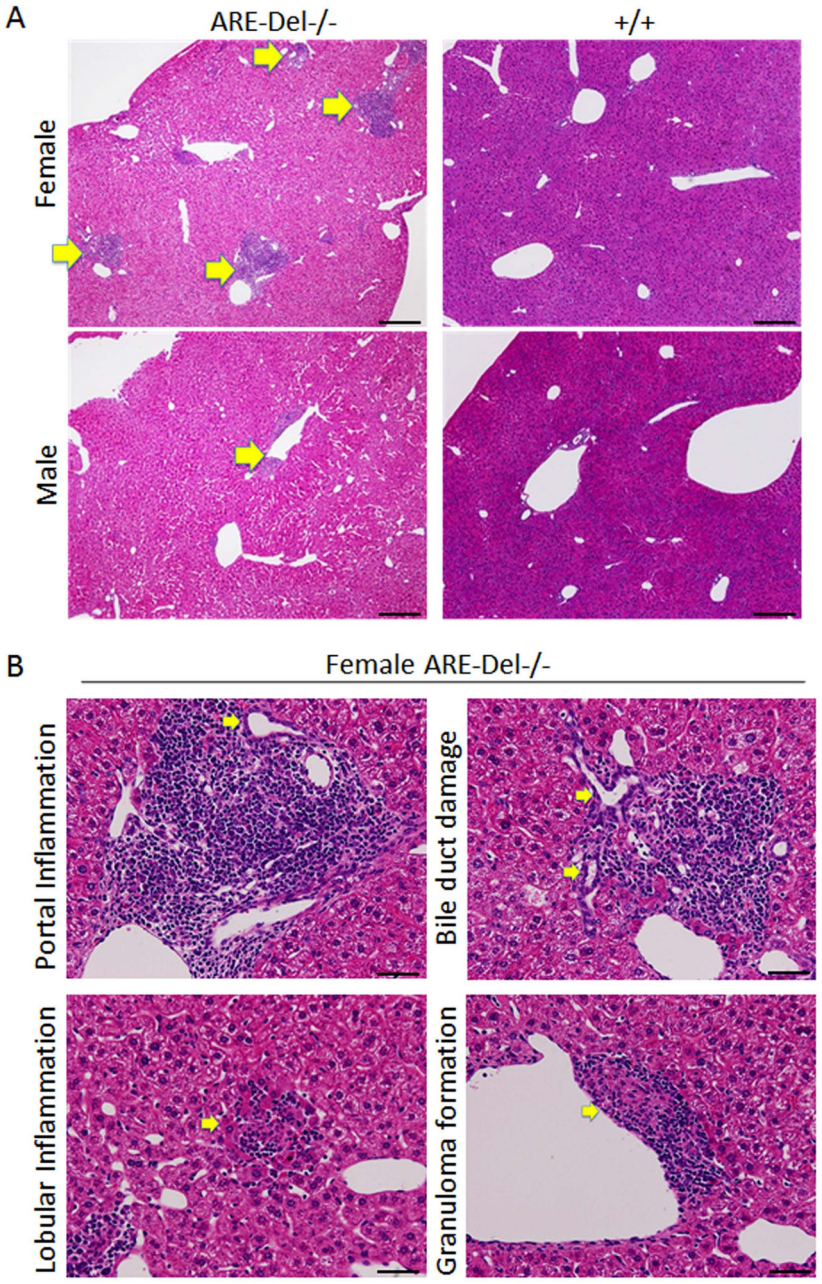

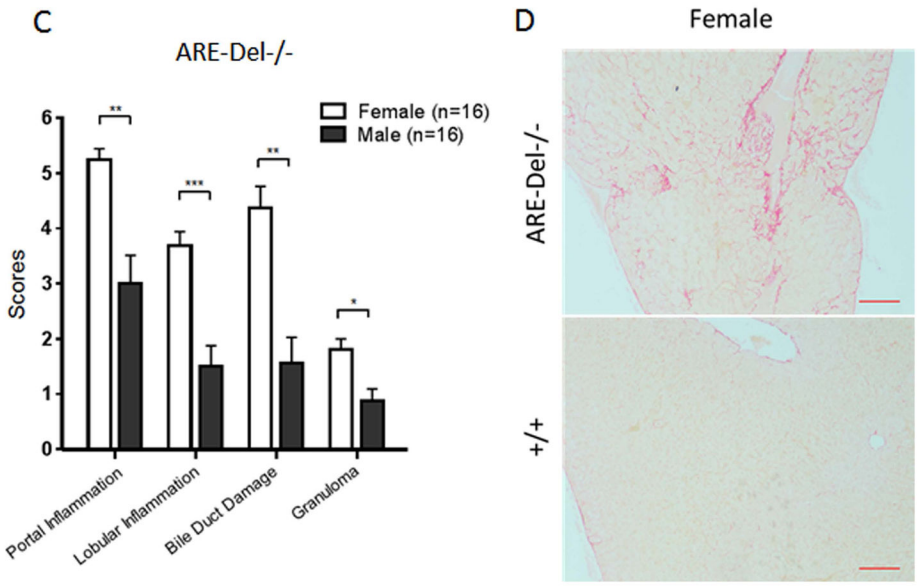

Figure 1.

Liver histology in ARE-Del−/− mice. 1A. Representative H&E staining of male and female ARE-Del−/− mice. Arrow bars point to the inflammatory foci region. 1B. Representative H&E staining of portal inflammation (arrow bar: bile duct showing mild damage), lobular inflammation (arrow bar: focal necrosis), biliary duct damage (arrow bar: bile duct showing moderate damage) and granuloma formation (arrow bar: epithelioid granuloma in portal tract) in female ARE-Del−/− mice. 1C. Statistical analysis of liver histology of male and female ARE-Del−/− mice was performed by the nonparametric Mann Whitney test using GraphPad Prism 6.0 (mean ± SEM; n=16 from three independent experiments). The two-tailed *p*-value < 0.05 was taken as significance (* $P < 0.05$, ** $P < 0.01$, *** $P < 0.001$, n.s., not significant). 1D. Representative Sirius Red staining of liver fibrosis in female ARE-Del −/− mice at age 20 wks. Scale bar: 200 μm (A left and D top); 50 μm (A right, B and D bottom).

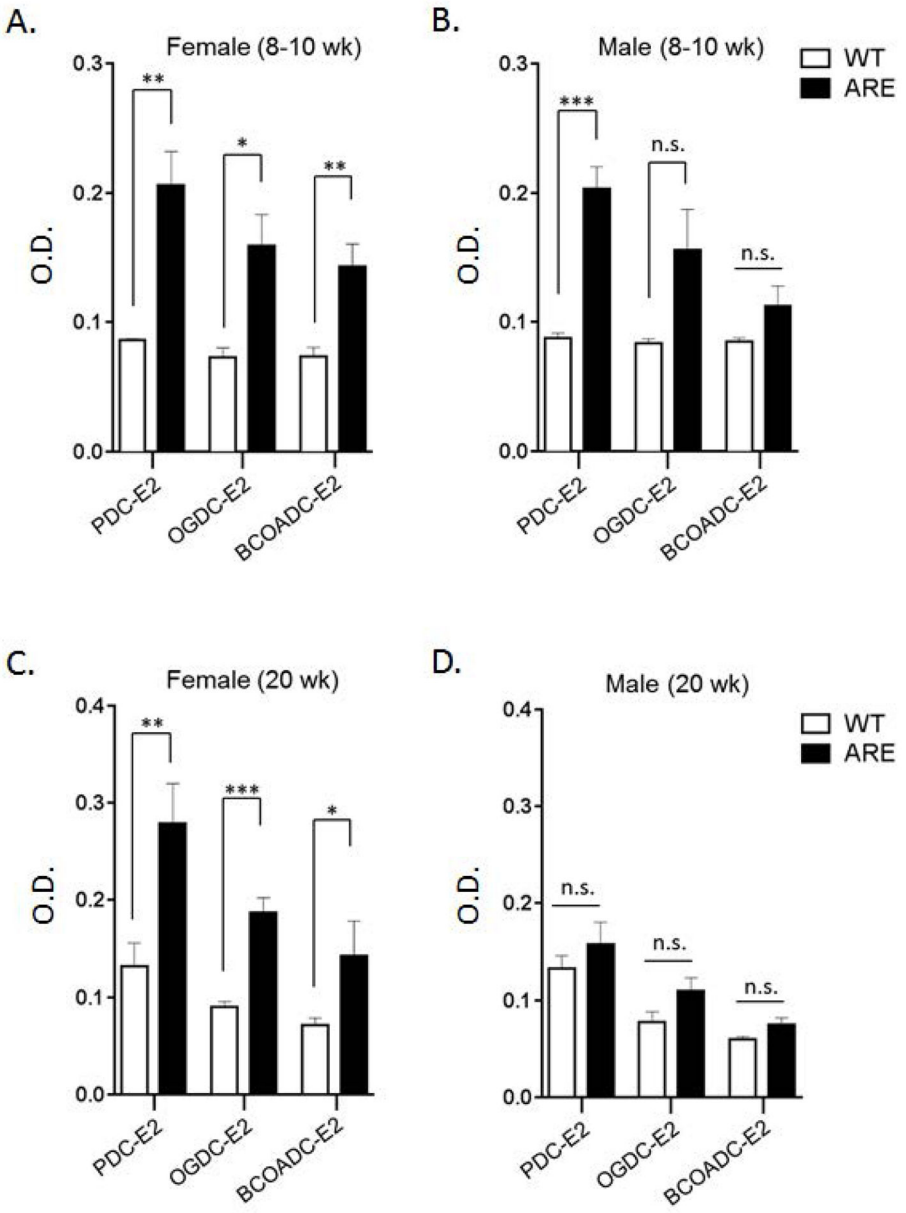

Figure 2.

Levels of anti-mitochondrial antibodies in ARE-Del−/− mice. 2A–B. Level of anti-PDC-E2, anti-OGDC-E2 and anti-BCOADC-E2 in the serum of female (A) and male (B) ARE-Del−/− at age 10 (±2) weeks (n=4). 2C–D. Level of anti-PDC-E2, anti-OGDC-E2 and anti-BCOADC-E2 in the serum of female (C) and male (D) ARE-Del−/− at age 20 (±2) weeks (n=7–8). Data represent mean ± SEM. Statistical analysis was performed by the unpaired Student's *t*-test. * $P < 0.05$, ** $P < 0.01$, *** $P < 0.001$, n.s., not significant. All data are representative of at least three independent experiments.

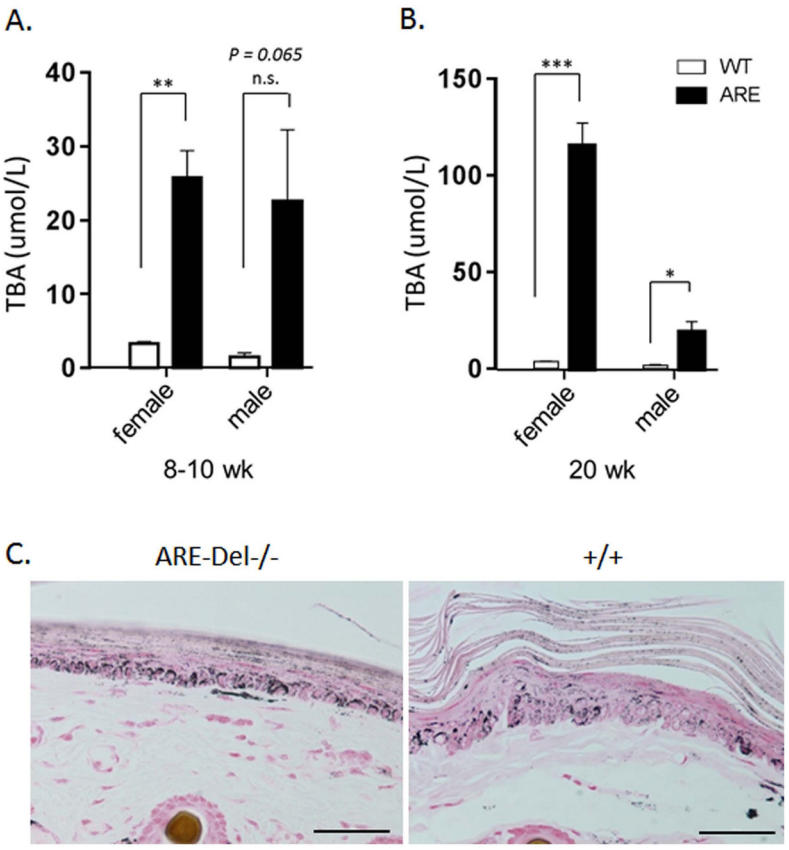

Figure 3.

Serum TBA levels in ARE-Del−/− mice. 3A. Serum TBA levels in female and male ARE-Del at age 10 (±2) weeks (n=4). 3B. Serum TBA levels in female and male ARE-Del at age 20 (±2) weeks (n=7–8). Data represent mean ± SEM. Statistical analysis was performed by the unpaired Student's *t*-test. * $P < 0.05$, ** $P < 0.01$, *** $P < 0.001$, n.s., not significant. 3C. Increased tail skin pigmentation in female ARE-Del−/− mice. All data are representative of at least three independent experiments.

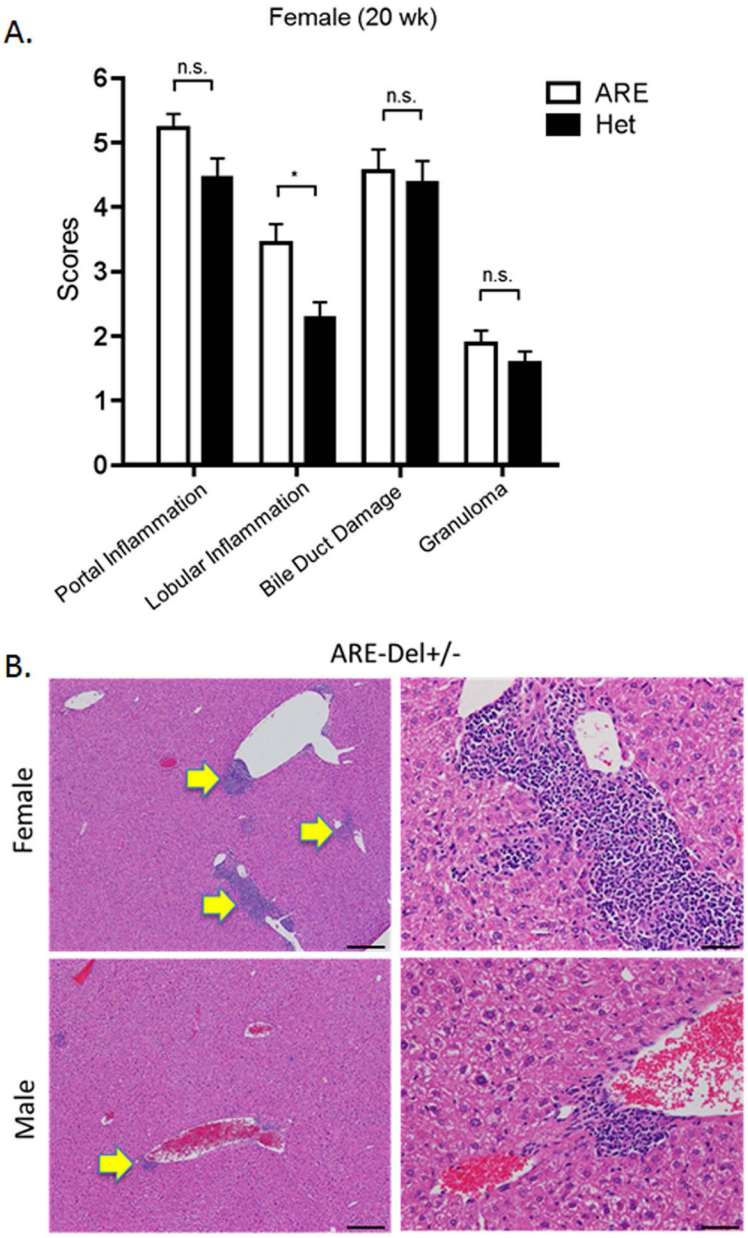

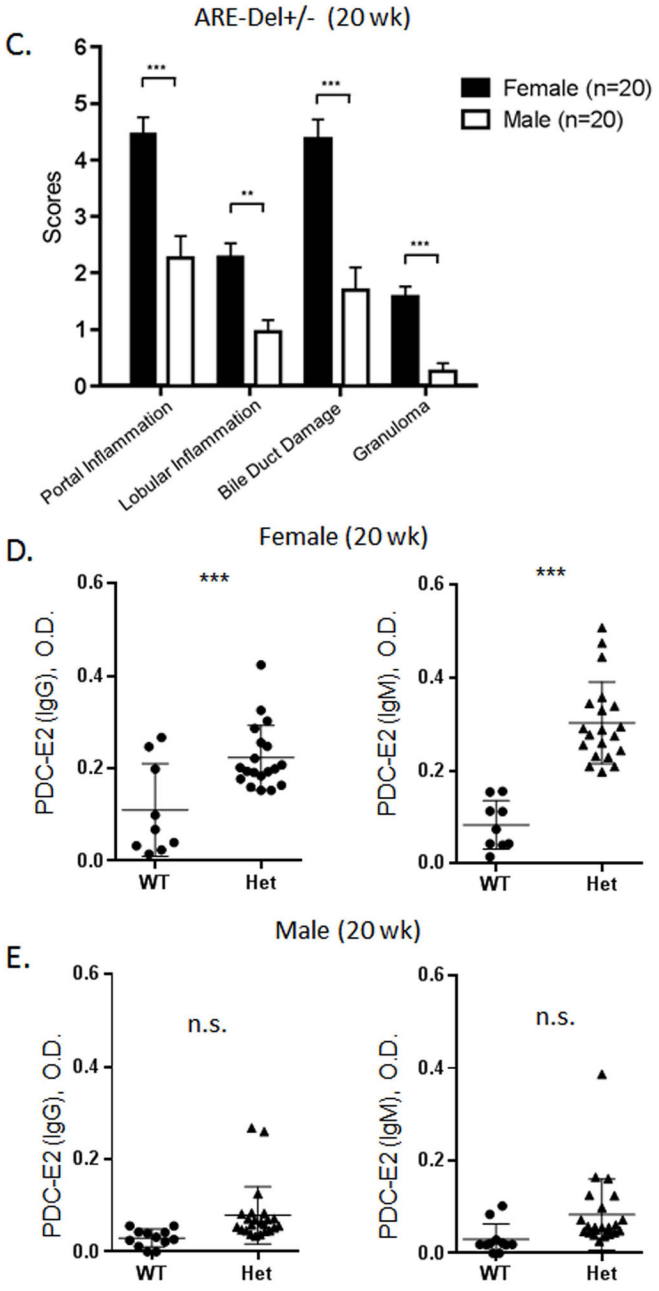

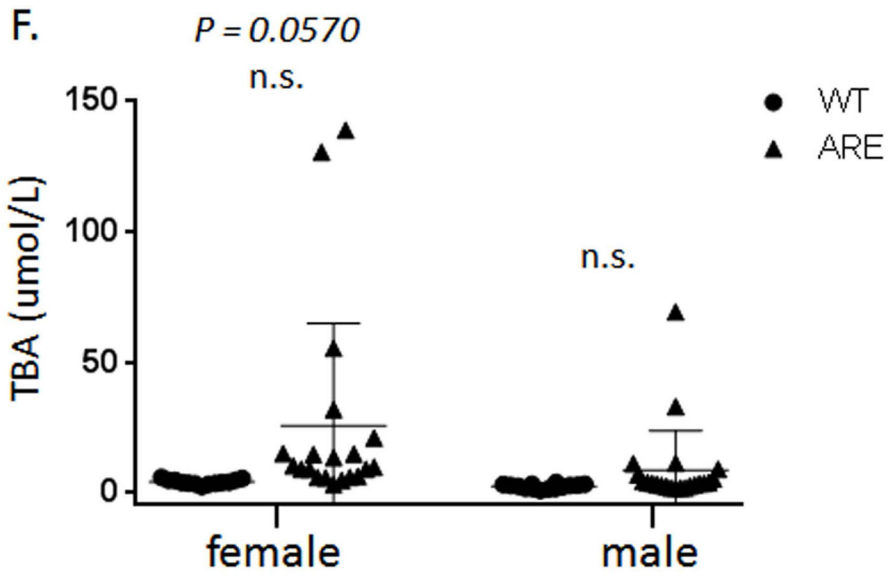

Figure 4.

Pathology of ARE-Del heterozygotes vs homozygotes. 4A. Statistical analysis of female ARE-Del−/− (n=9 from two independent experiments) vs ARE-Del+/− mice (n=23 from two independent experiments) in portal inflammation, lobular inflammation, biliary damage and granuloma formation at age 20 wks (mean ± SEM), performed by nonparametric Mann Whitney test with the two-tailed *p*-value. 4B. Representative H&E staining of male and female ARE-Del+/− mice at age 20 wks. Arrow bars point to the inflammatory foci region. 4C. Statistical analysis of liver histology of male and female ARE-Del+/− mice (n=20 ± 2 from two independent experiments) was performed by Mann Whitney test with the two-tailed *p*-value. 4D–E. IgG and IgM anti-PDC-E2 in male and female ARE-Del+/− mice at age 20 wks (mean ± SD, n=20 ± 2). 4F. Serum TBA in male and female ARE-Del+/− mice at age 20 wks (mean ± SD, n=20 ± 2). 4D–F. Statistical analysis was performed by the unpaired Student's *t*-test.* $P < 0.05$, ** $P < 0.01$, *** $P < 0.001$, n.s., not significant.

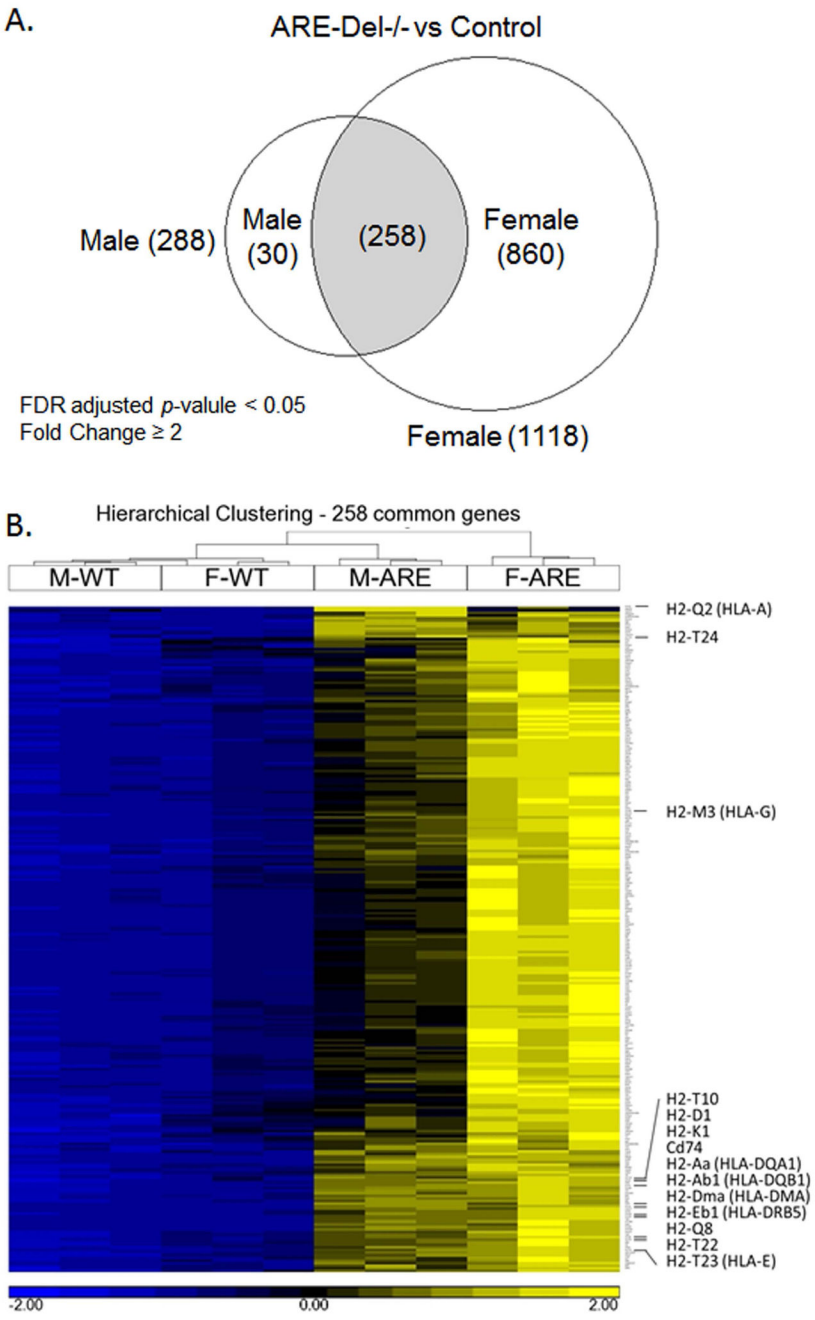

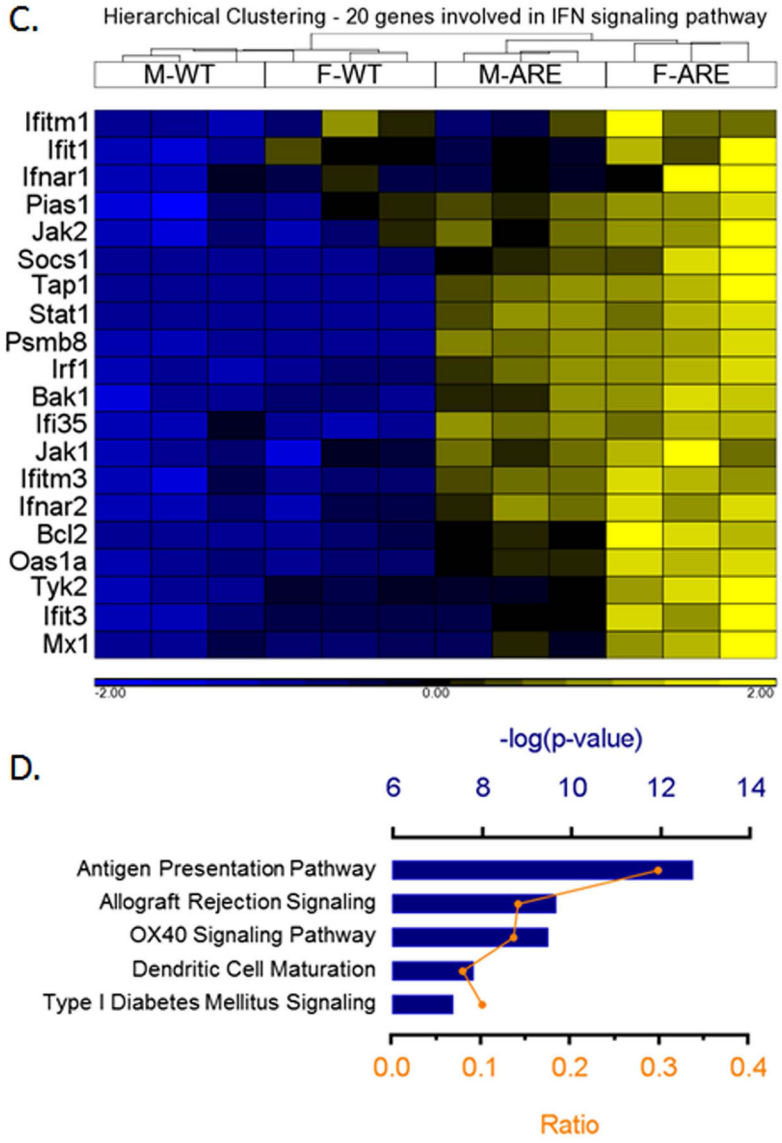

Figure 5.

Hepatic gene expression in male and female ARE-Del−/− mice at age 20 wks. 5A. Venn diagram of differentially expressed genes in male and female ARE-Del−/− mice vs control mice (n=3). 5B. Hierarchical clustering of 258 common genes. The human homologs are described in parentheses. 5C. Hierarchical clustering of 20 genes involved in interferon signaling pathway. 5D. Top canonical pathways of common genes derived from IPA. Ratio (bottom y-axis, yellow line) refers to the number of genes from dataset divided by the total number of genes that make up that pathway from within the IPA knowledgebase and the -log of *P* value (top y-axis, bar) was calculated by Fisher's exact test.

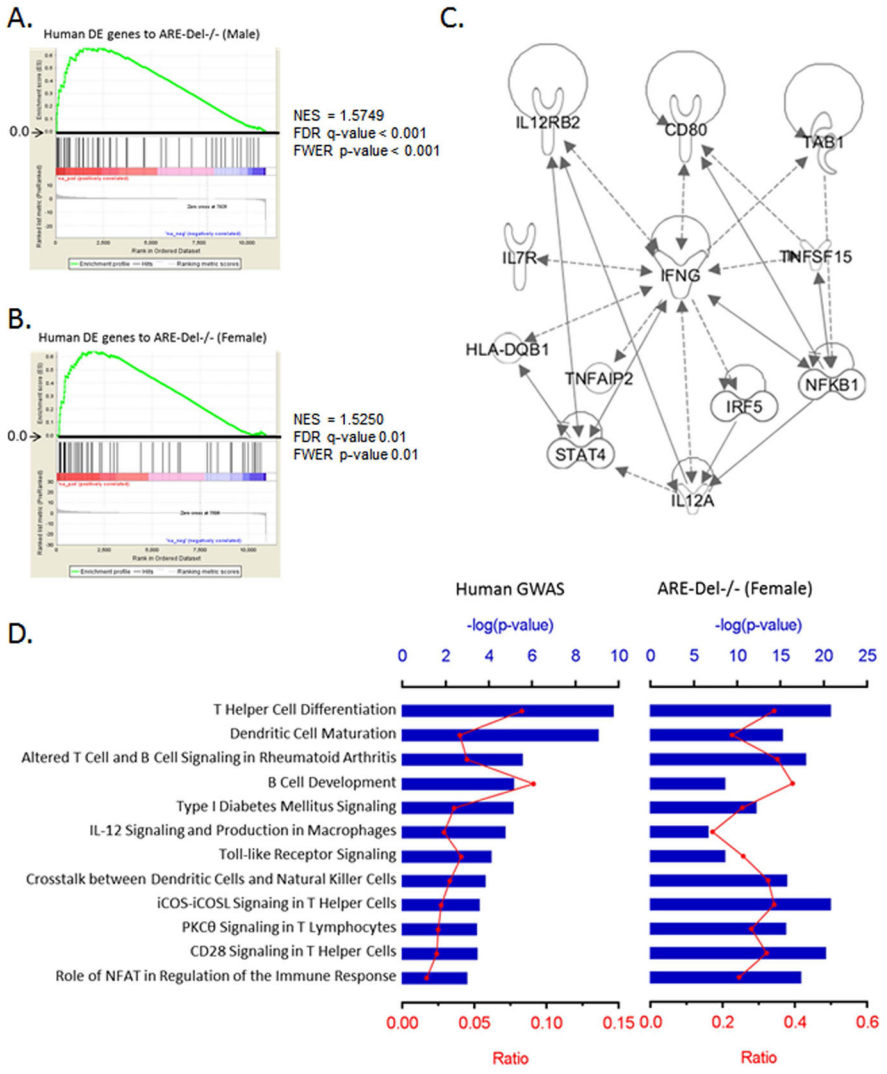

Figure 6.

Comparison of the gene expression profiling to human data from PBC patients. 6A–B. GSEA enrichment plots for human DE genes in PBC-BEC lesions using gene sets of male (A) and female (B) ARE-Del−/− mice. NES; normalized enrichment scores, FDR; false discovery rate, FWER; family-wise error rate. 6C. Top network identified by IPA for the most significant 26 variants. The lines between genes represent known interactions (solid line for direct interaction; dashed line for indirect interaction). 6D. Canonical pathways of human GWAS with ARE-Del−/− mice. The most significant 26 variants were selected by the NHGRI GWAS catalog ($p \leq 1 \times 10^{-5}$). Top canonical pathways of these genes were derived from ingenuity pathway analysis (IPA) and compared with ones from female ARE-Del−/− mice. Ratio (bottom y-axis, yellow line) refers to the number of genes from dataset divided by the total number of genes that make up that pathway from within the IPA knowledgebase and the -log of *P* value (top y-axis, bar) was calculated by Fisher's exact test.

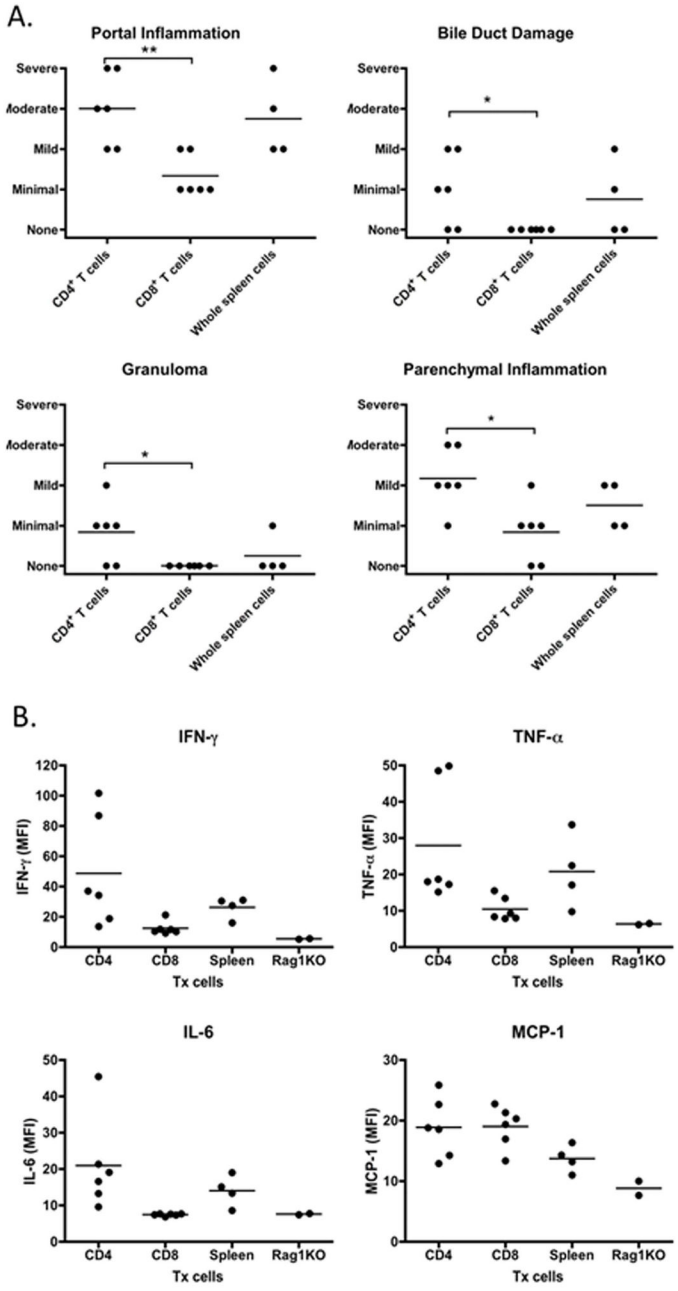

Figure 7.

Liver histopathology and level of inflammatory cytokines in recipient mice. 7A. Pathological score of portal inflammation, bile duct damage, granuloma and parenchymal inflammation and bile duct damage in group of $CD4^+$ T cell (n=6), $CD8^+$ T cells (n=6) and whole spleen cells (n=4) recipient mice. 7B. Serum were collected 20 weeks after cell transfer, the levels of IFN-, TNF-α, IL-6 and MCP-1 in group of $CD4^+$ T cell (n=6), $CD8^+$ T cells (n=6) and whole spleen cells (n=4) recipient mice were measured by a mouse inflammatory cytokine

CBA kit. *, $p < 0.05$; **, $p < 0.01$, determined using Kruskal-Wallis Test (Nonparametric ANOVA). All data are representative of at least two independent experiments.

Table 1

Upregulation of MHC class I and II genes in ARE-Del−/− mice

		ARE-Del−/− (Male)		ARE-Del−/− (Female)	
MHC	**Gene**	***p*-value**	**Fold**	***p*-value**	**Fold**
Class II	Cd74	1.54×10^{-5}	44.5	6.26×10^{-6}	37.4
	H2-DMa	3.64×10^{-4}	40.6	5.55×10^{-5}	33.7
	H2-Aa	2.96×10^{-4}	34.1	7.95×10^{-5}	30.0
	H2-Eb1	1.97×10^{-4}	27.0	1.69×10^{-5}	30.0
	H2-Ab1	1.26×10^{-4}	21.1	1.48×10^{-5}	22.5
Class I	H2-Q2	1.57×10^{-6}	23.7	3.0×10^{-3}	4.4
	H2-Q8	2.95×10^{-4}	4.8	4.65×10^{-5}	3.9
	H2-M3	9.19×10^{-6}	4.1	1.48×10^{-7}	4.3
	H2-T10	1.69×10^{-5}	3.9	2.34×10^{-5}	2.6
	H2-T23	8.59×10^{-6}	3.8	1.59×10^{-6}	3.2
	H2-D1	7.44×10^{-8}	3.2	1.88×10^{-8}	3.1
	H2-K1	4.89×10^{-7}	3.0	4.80×10^{-7}	2.5
	H2-T24	9.70×10^{-4}	2.8	2.41×10^{-4}	2.0
	H2-T22	2.90×10^{-5}	2.7	6.23×10^{-6}	2.4